

bond. This is a remarkably simple counterexample to the prevailing hope that a crystal structure describes the solution structure.

There is no intramolecular hydrogen bond in aqueous hydrogen succinate monoanion (9). Yet in THF this shows only the intrinsic isotope shift. Therefore the conformation must have changed, to permit a hydrogen bond that is not only intramolecular but also symmetric. In such a nonpolar solvent, the best solvation for the carboxylate anion is hydrogen bonding to a carboxylic acid. Moreover, the symmetry of this hydrogen bond in THF is further evidence for a role for solvation in determining the symmetry of hydrogen bonds.

These results do not distinguish whether hydrogen bonds become asymmetric in water because of its polarity or because of its disorder. Certainly a polar environment ought to stabilize the asymmetric structure, with its concentrated negative charge, relative to the symmetric one, with delocalized charge. The MO calculations mentioned above²³ show that polarity does favor the asymmetric structure, but Hadži suggests that if the dynamic and discrete properties of water are included, this structure would be even more favored. It seems to us that polarity alone is not sufficient, since the crystal, with its counterions, is also quite polar, and yet the hydrogen bond is symmetric. Therefore we infer that the hydrogen bonds become asymmetric in water because of its disorder, which makes it improbable for both carboxyls to be identically solvated at each instant.

Conclusions

The hydrogen bonds in aqueous hydrogen succinate (9), maleate (5), and phthalate (6) monoanions are asymmetric, corresponding to a potential-energy surface having two minima. This conclusion is based on the values of K_T calculated from observed isotope shifts, the temperature dependence of the isotope shift, and the unusual isotope shifts of the aromatic carbons of phthalic acid, which are not subject to an intrinsic shift. The results on hydrogen maleate and phthalate are especially surprising since they had previously been observed to have symmetric hydrogen bonds. This difference is attributed to the disorder of the aqueous environment. In contrast, in nonpolar solvents single-well potentials are observed, not only for hydrogen maleate and phthalate monoanions, but also for hydrogen succinate.

Whether a hydrogen bond is symmetric or asymmetric is not simply inherent in the molecular structure, dependent only on the oxygen-oxygen distance, but can depend on solvent. The technique of isotopic perturbation of equilibrium has demonstrated itself to be a useful and effective technique in the study of hydrogen bonding, and it provides definitive answers to the question of the symmetry of the hydrogen bond.

Acknowledgment. This research was supported by National Science Foundation Grant CHE90-25113. Purchase of the 500-MHz NMR spectrometer was made possible by NIH Grant RR04733 and NSF Grant CHE88-14866.

Theoretical Secondary Kinetic Isotope Effects and the Interpretation of Transition State Geometries. 1. The Cope Rearrangement

K. N. Houk,* Susan M. Gustafson,[†] and Kersey A. Black

Contribution from the Department of Chemistry and Biochemistry, University of California, Los Angeles, Los Angeles, California 90024-1569. Received March 30, 1992

Abstract: Theoretical secondary kinetic and equilibrium deuterium isotope effects for the Cope rearrangement of 1,5-hexadiene were calculated using RHF/3-21G, RHF/6-31G*, UHF/6-31G*, CASSCF/3-21G, and MP2/6-31G* levels of theory and the Bigeleisen-Mayer method. Isotope effects for transition structures, corresponding to a concerted process of bond reorganization, several different cyclohexane-1,4-diyl-like species, and two allyl radicals, were examined and compared with the experimentally determined values. The theoretical isotope effects calculated for the concerted pathway are in best agreement with experiment. Similar calculations were used to examine the 1,5-heptadiene and 3-methyl-1,5-hexadiene Cope rearrangements. The transition structure with methyl in the equatorial position is 1–2 kcal/mol more stable than that with the axial methyl. These results are analyzed in the framework of Gajewski's More O'Ferrall-Jencks diagrams for the Cope rearrangement, correlating kinetic isotope effects and bond order.

Introduction

The Cope [3,3]-sigmatropic rearrangement has been the subject of extensive theoretical and experimental investigations.^{1–3} This class of reactions is generally thought to proceed by a concerted mechanism, but this point is still debated. Even those who agree that the rearrangement is concerted sometimes disagree regarding the geometry of the transition state. Some investigators favor a cyclohexane-1,4-diyl-like structure (bottom of Figure 1), while others support a so-called "aromatic" transition state consisting of two partially bonded three-carbon units (center of Figure 1). Two separated allyl radicals (top of Figure 1) are known to be too high in energy to qualify as participants in this reaction but do represent another limiting structure useful to this discussion. The best computational evidence available predicts a potential surface with two pathways, one via an aromatic transition state, the other through a cyclohexanediyl intermediate. Both pathways

have identical energies.²⁸ Calculation of free energies leads to the prediction that both pathways are concerted and that the

- (1) (a) Cope, A. C.; Hardy, E. M. *J. Am. Chem. Soc.* **1940**, *62*, 441–44. (b) Doering, W. v. E.; Roth, W. R. *Tetrahedron* **1962**, *67–74*. (c) Zimmerman, H. E. *J. Am. Chem. Soc.* **1966**, *88*, 1564–65. (d) Frey, H. M.; Walsh, R. *Chem. Rev.* **1969**, *69*, 103–124. (e) Doering, W. v. E.; Toscano, V. G.; Beasley, G. H. *Tetrahedron* **1971**, *27*, 5299–5306. (f) Rhoads, S. J.; Rawlins, R. N. *Org. React.* **1975**, *22*, 1–251. (g) Wehrli, R.; Schmid, H.; Bellus, D.; Hansen, H.-J. *Helv. Chim. Acta* **1977**, *60*, 1325–56. (h) Dewar, M. J. S.; Wade, L. E. *J. Am. Chem. Soc.* **1973**, *95*, 290–291; **1977**, *99*, 4417–24. (i) Doering, W. v. E. *Proc. Natl. Acad. Sci. U.S.A.* **1981**, *78*, 5279–83. (j) Frey, H. M.; Solly, R. K. *Trans. Faraday Soc.* **1968**, *64*, 1858. (2) (a) Kormornicki, A.; McIver, J. W. *J. Am. Chem. Soc.* **1976**, *98*, 4553–61. (b) Osamura, Y.; Kato, S.; Morokuma, K.; Feller, D.; Davidson, E. R.; Borden, W. T. *J. Am. Chem. Soc.* **1984**, *106*, 3362–63. (c) Morokuma, K.; Borden, W. T.; Hrovat, D. A. *J. Am. Chem. Soc.* **1988**, *110*, 4474–75. (d) Borden, W. T.; Loncharich, R. J.; Houk, K. N. *Annu. Rev. Phys. Chem.* **1988**, *39*, 213–36. (e) Bearpark, M.; Bernardi, F.; Olivucci, M.; Robb, M. A. *J. Am. Chem. Soc.* **1990**, *112*, 1732–1737. (f) Borden, W. T.; Hrovat, D. A.; Vance, R. L.; Rondan, N. G.; Houk, K. N.; Morokuma, K. *J. Am. Chem. Soc.* **1990**, *112*, 2018–19. (g) Dupuis, M.; Murray, C.; Davidson, E. R. *J. Am. Chem. Soc.* **1991**, *113*, 9756–9759.

[†] Nē Susan M. Ernst.

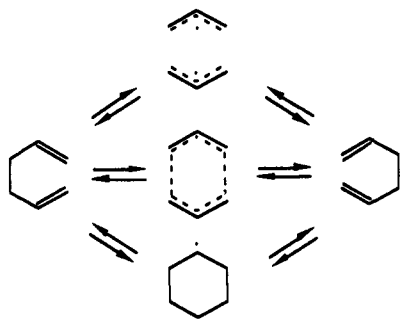


Figure 1. The allyl radical, synchronous concerted, and 1,4-diyli pathways for the Cope rearrangement of 1,5-hexadiene.

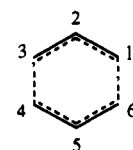
aromatic concerted pathway is 2 kcal/mol below the 1,4-diyli concerted pathway.

We have employed several levels of ab initio molecular orbital theory to generate different plausible transition state structures for the Cope reaction and to calculate theoretical secondary kinetic isotope effects for reactions involving each of these structures. This, rather than further structural computations, has been carried out for two reasons. First, kinetic secondary deuterium isotope effects have long been recognized as a sensitive probe of geometric changes occurring in the transition state. A concordance between experimental and theoretical isotope effects is taken as validation of a particular transition structure and corresponding mechanistic pathway. This approach has proved fruitful in the investigation of several types of pericyclic reactions.⁴ Second, although the relationship between bond force constants and isotope effects is well-known and indeed has been used to estimate qualitatively the extent of bond formation in the transition state, the relationship is also complex.⁵ A relatively simple quantitative relationship between secondary kinetic isotope effects and geometric parameters, such as bond strength or bond length, would be useful if it can be developed. Crucial to its development is establishing the geometry of transition state structures for reactions for which the kinetic secondary isotope effects are known. In this paper we report the theoretical geometric parameters and kinetic isotope effects for the Cope rearrangement of 1,5-hexadiene and several methyl substituted derivatives. In subsequent publications this approach will be applied to the Cope and Claisen rearrangements of other unsaturated systems and substituted compounds.⁶

Background

Secondary Isotope Effects. A number of methods have been developed for calculating theoretical secondary isotope effects. One approach relies on a force field parameterized from experimental vibrational frequencies for small molecules. The force field is used to compute "fractionation factors", which are equilibrium isotope effects for the partitioning of deuterium between sites in structures at equilibrium.⁷ These fractionation factors are then used to predict equilibrium isotope effects for

Table I. Transition State Energies and Carbon-Carbon Bond Lengths for the Cope Transition State of 1,5-Hexadiene

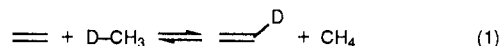


level of theory	ΔE^\ddagger (kcal/mol)	C(1)-C(6) (Å)	C(1)-C(2) (Å)
RHF/3-21G	45.9	2.020	1.389
RHF/6-31G*	56.6	2.046	1.390
RMP2/6-31G**a	31.4	2.046	1.390
CASSCF/3-21G ^c	40.7	2.086	1.401
CASSCF/6-31G**d	47.7	2.189	1.398

^aOn RHF/6-31G* optimized geometries. ^bSix orbitals and six electrons including the 12 most important configurations.^{2b} ^cSix orbitals and six electrons.^{2c} ^dSix orbitals and six electrons.^{2d}

larger molecules of interest by structural analogy.

Isotope effects can also be calculated using force constants derived from ab initio molecular orbital calculations.⁸ Hout and co-workers used theoretical force constants to calculate the reduced isotopic partition functions and equilibrium isotope effects for a number of small molecules.^{8a} They then compared these quantities with the corresponding values derived from spectroscopic data. For example, calculation of the H/D exchange reaction involving ethylene and monodeuteriomethane, eq 1, at the RHF/3-21G, RHF/6-31G*, and MP2/6-31G* levels of theory gave equilibrium constants of 0.87, 0.84, and 0.75, respectively, with deuterium concentrating at the sp³ center. The corresponding equilibrium



constant derived from spectroscopic data, with and without the removal of anharmonicity, is 0.78 and 0.82, respectively.

Hess and Schaad have calculated the secondary isotope effects for the electrocyclic ring closure of (Z)-1,3,5-hexatriene and the ring opening of cyclobutene using ab initio quantum mechanical calculations at the RHF/6-31G* and MP2/6-31G* levels, respectively.⁴ Good correlations with experiment were obtained.

Saunders, Laidig, and Wolfsberg have recently released a program, QUIVER,⁹ which conveniently calculates theoretical secondary isotope effects from force constants determined through ab initio calculations. The fundamental theory from which the isotope effects are calculated was derived by Bigeleisen and Mayer¹⁰ and is based upon transition state theory.¹¹ In this procedure, the geometry of each structure is optimized using ab initio methodology and subjected to a completed vibrational analysis, and the resulting molecular geometry and Cartesian force constant matrix are used with the program QUIVER to compute the reduced isotopic partition function, $(s_2/s_1)_f$, shown in eq 2. Equilibrium isotope effects are computed by dividing the reduced isotopic partition function of the reactant by that of the product. Kinetic isotope effects are obtained in a similar manner by dividing the reduced isotopic partition function of the reactant by that of the transition state. This ratio is then multiplied by the ratio of the imaginary frequencies in the undeuterated and deuterated

(3) (a) Dewar, M. J. S.; Ford, G. P.; McKee, M. L.; Zepa, H. R.; Wade, L. E. *J. Am. Chem. Soc.* **1977**, *99*, 5069-73. (b) Dewar, M. J. S.; Healy, E. F. *J. Phys. Lett.* **1987**, *141*(6), 521-24. (c) Dewar, M. J. S.; Jie, C. *J. Am. Chem. Soc.* **1987**, *109*, 5893-900. (d) Dewar, M. J. S.; Jie, C. *J. Chem. Soc., Chem. Commun.* **1987**, 1451-53. (e) Dewar, M. J. S.; Jie, C. *J. Chem. Soc., Chem. Commun.* **1989**, 98-100.

(4) (a) Baldwin, J. E.; Reddy, P. V.; Hess, B. A., Jr.; Schaad, L. J. *J. Am. Chem. Soc.* **1988**, *110*, 8554-55. (b) 8555.

(5) (a) Gajewski, J. J.; Conrad, N. D. *J. Am. Chem. Soc.* **1979**, *101*, 6693-6704. (b) Gajewski, J. J. *J. Am. Chem. Soc.* **1979**, *101*, 4393-94. (c) Gajewski, J. J.; Conrad, N. D. *J. Am. Chem. Soc.* **1978**, *100*, 6268-69, 6269-70. (d) Gajewski, J. J.; Emrani, J. *J. Am. Chem. Soc.* **1984**, *106*, 5733-34. (e) Gajewski, J. J. *Acc. Chem. Res.* **1980**, *13*, 142-55. (f) Gajewski, J. J. In *Isotopes in Organic Chemistry*; Buncl, E., Ed.; Elsevier: New York, 1987; Chapter 3, Vol. I.

(6) Gustafson, S. M.; Black, K. A.; Houk, K. N., manuscript in preparation.

(7) (a) Hartshorn, S. R.; Shiner, V. J., Jr. *J. Am. Chem. Soc.* **1972**, *94*, 9002-12. (b) Budenbaum, W. E.; Shiner, V. J., Jr. *ACS Symp. Ser.* **1975**, *11*, 163. Shiner, V. J., Jr.; Neumann, T. E. *Z. Naturforsch., A: Phys. Sci.* **1989**, *44*, 3-37.

(8) (a) Hout, R. F., Jr.; Levi, B. A.; Hehre, W. J. *J. Comput. Chem.* **1982**, *3*(2), 234-50. (b) Hehre, W. J.; Radom, L.; Schleyer, P. v. R.; Pople, J. A. *Ab Initio Molecular Orbital Theory*; John Wiley and Sons: New York, 1986. (c) Pople, J. A.; Schlegel, H. B.; Krishnan, R.; Defrees, D. J.; Binkley, J. S.; Frisch, M. J.; Whiteside, R. A.; Hout, R. F.; Hehre, W. J. *Int. J. Quantum Chem., Quantum Chem. Symp.* **1981**, *15*, 269-78.

(9) Saunders, M.; Laidig, K. E.; Wolfsberg, M. *J. Am. Chem. Soc.* **1989**, *111*, 8989-94.

(10) (a) Bigeleisen, J.; Mayer, M. G. *J. Chem. Phys.* **1947**, *15*, 261-67. (b) Bigeleisen, J.; Wolfsberg, M. *Adv. Chem. Phys.* **1958**, *1*, 15. (c) Wolfsberg, M.; Stern, M. *J. Pure Appl. Chem.* **1964**, *8*, 225. (d) Bigeleisen, J. *J. Chem. Phys.* **1949**, *17*, 675.

(11) Glasstone, S.; Laidler, K. J.; Eyring, H. *The Theory of Rate Processes*; McGraw-Hill: New York, 1941.

transition states, as expressed in eq 3.

$$\left(\frac{s_2}{s_1}\right) f_{GS} = \prod_{i=1}^{3N-6} \frac{u_{2i}}{u_{1i}} \prod_{i=1}^{3N-6} \frac{[1 - e^{-u_{1i}}]}{[1 - e^{-u_{2i}}]} \exp\left[\frac{\sum (u_{1i} - u_{2i})}{2}\right] \quad (2)$$

$$\frac{k_H}{k_D} = \frac{\nu_{1L}^* (s_2/s_1) f_{GS}}{\nu_{2L}^* (s_2/s_1) f_{TS}} \quad (3)$$

$$u_i = h\nu_i/kT$$

For transition states the $3N - 6$ is changed to $3N - 7$. Due to errors such as the neglect of anharmonicity, it is common practice to scale vibrational frequencies.¹²

Cope Rearrangement. The [3,3]-sigmatropic rearrangement of 1,5-hexadiene occurs with an experimental activation enthalpy of 33.5 kcal/mol and an entropy of activation of -13.8 eu.^{1d} Ab initio quantum mechanical calculations on this reaction have been carried out by several groups, and a few of these results are summarized in Table I.^{2,3} These calculations support experimental evidence that the transition structure prefers a chair-like conformation of C_2 symmetry. The RHF and CASSCF structures are in close agreement, with breaking and forming bond lengths of 2.0–2.2 Å.^{2c}

Very recent results of Dupuis et al. with MCSCF calculations and the 6-31G* basis set predict a chair-like C_2 transition structure, which has the lowest free energy, but a C_2 1,4-diyl intermediate is only slightly higher in energy.^{2b} A natural orbital analysis that we carried out on the CASSCF/3-21G wave function for the 1,4-diyl species indicates that it has only 10–15% more diradical character than the ground state and is predominantly a closed-shell species.^{2b} A true 1,4-diyl species was found to be significantly higher in energy than the concerted transition state by this calculation.¹³ Transition state energies have been commonly calculated relative to the C_1 symmetric conformation of 1,5-hexadiene.¹⁴

Results and Discussion

Transition State Structures and Energetics. In this study, all structures were optimized to stationary points on the potential energy surface and were subjected to a frequency analysis using either the GAUSSIAN¹⁵ or GAMESS¹⁶ series of programs. All vibrational frequencies were scaled to account for anharmonicity. Specifically, frequencies calculated at the RHF/3-21G¹⁷ level were reduced by 10%, the RHF/6-31G*¹⁸ frequencies were reduced by 13%, and the MP2/6-31G*¹⁹ frequencies were reduced by 7%.

(12) (a) Hess, A. B., Jr.; Schaad, L. J. *Chem. Rev.* **1986**, *86*, 709–30. (b) Wolfsberg, M.; Hout, R. F., Jr.; Hehre, W. J. *Am. Chem. Soc.* **1980**, *102*, 3296–98.

(13) Previous work found a singlet diradical species optimized at the CASSCF/3-21G level to be 22 kcal/mol higher in energy than the concerted transition structure.^{2c} Our unpublished results found the singlet diradical to be higher in energy also, but at most only by 7 kcal/mol CASSCF/3-21G/UHF/3-21G (6 electron and 6 orbital active space).

(14) 1,5-Hexadiene is commonly optimized under C_1 symmetry constraints, but C_2 symmetric 1,5-hexadiene is at some levels of theory very slightly lower in energy (e.g., by 0.1 kcal/mol at the RHF/6-31G* level). While not significantly affecting the calculated energy of the transition state, it is a potential concern when calculating theoretical isotope effects. Isotope effects calculated using a C_2 ground state structure were found to be insignificantly different from those proceeding from the C_1 symmetry species.

(15) (a) Frisch, M. J.; Binkley, J. S.; Schlegel, H. B.; Raghavachari, K.; Martin, R.; Stewart, J. J. P.; Bobrowicz, F.; DeFrees, D. J.; Seeger, R.; Whiteside, R.; Fox, D.; Fluder, E. M.; Pople, J. A. GAUSSIAN 86, Release C. Department of Chemistry, Carnegie Mellon University, Pittsburgh, PA. (b) Frisch, M. J.; Head-Gordon, M.; Schlegel, H. B.; Raghavachari, K.; Binkley, J. S.; Gonzalez, C.; DeFrees, D. J.; Fox, D.; Seeger, R.; Whiteside, R.; Melius, C. F.; Baker, J.; Martin, R.; Kahn, L. R.; Stewart, J. J. P.; Fluder, E. M.; Topiol, S.; Pople, J. A. GAUSSIAN 88; GAUSSIAN, Inc.: Pittsburgh, PA, 1988.

(16) Dupuis, M.; Spangler, D.; Wendolowski, J. J. *NRCC Software Catalog*, Vol. 1, 1980, Program CG01 (GAMESS).

(17) Binkley, J. S.; Pople, J. A.; Hehre, W. J. *J. Am. Chem. Soc.* **1980**, *102*, 939.

(18) Hehre, W. J.; Ditchfield, R.; Pople, J. A. *J. Chem. Phys.* **1972**, *56*, 2257.

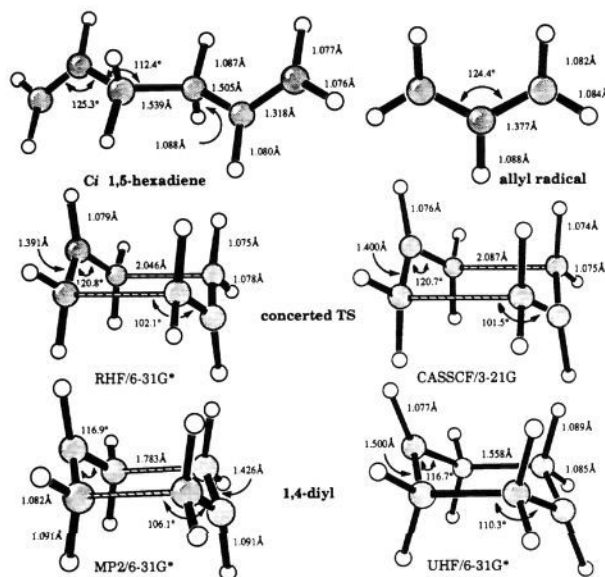


Figure 2. Optimized structures of C_1 1,5-hexadiene (RHF/6-31G*), the Cope concerted transition structure (RHF/6-31G* and CASSCF/3-21G), cyclohexane-1,4-diyl (MP2/6-31G* and UHF/6-31G*), and allyl radical (UHF/6-31G*).

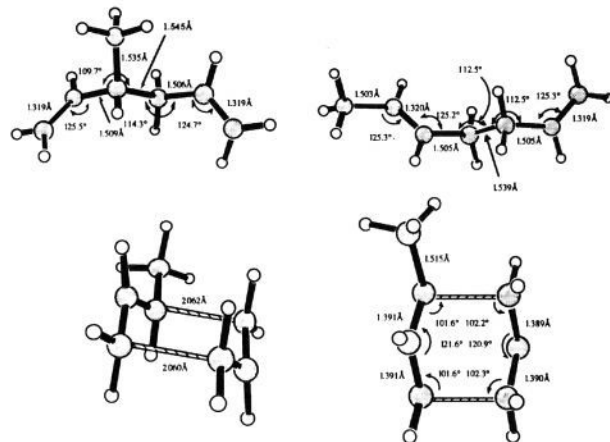


Figure 3. Optimized structures (RHF/6-31G*) of 3-methyl-1,5-hexadiene, *trans*-1,5-heptadiene, and the Cope concerted transition structure (two views).

The data thus obtained was used with the QUIVER program to calculate theoretical secondary deuterium isotope effects.

As a model for the concerted aromatic transition state of the Cope rearrangement of 1,5-hexadiene, a C_2 symmetric chair conformation, optimized to a stationary point at the RHF/3-21G, RHF/6-31G*, and CASSCF/3-21G levels was used. These three calculations provide very similar structures, with bond-breaking and bond-forming distances of 2.0–2.1 Å. Vibrational analysis with these wave functions revealed each of the stationary points so determined to be a transition state with a single negative eigenvalue.

In contrast to RHF methodology, which underestimates radical stability, UHF and MP2 calculations overestimate the stability of diradicals.^{2f} A C_2 symmetric cyclohexane-1,4-diyl singlet diradical, with a C(1)–C(6) bond distance of 1.558 Å was located as a minimum on the UHF/6-31G* potential energy surface. At the MP2/6-31G* level, a 1,4-diyl stationary point 28.6 kcal/mol higher in energy than 1,5-hexadiene was located. Vibrational analysis of this structure at the MP2/6-31G* level again revealed no imaginary frequencies; it is a potential energy minimum, and not a transition state. This and the intermediate bond-forming

(19) Möller, C.; Plesset, M. S. *Phys. Rev.* **1934**, *46*, 618.

Table II. Energies^a and Relative Energies^b for Transition Structures of the Cope Rearrangement of 3-Methyl-1,5-hexadiene with Methyl in the Axial and Equatorial Positions

level of theory	<i>E</i> (CH ₃ axial)	<i>E</i> (CH ₃ equatorial)	ΔE
RHF/3-21G	-270.436 14	-270.439 25	1.95
RHF/6-31G ^{cc}	-271.925 00	-271.928 28	2.06
MP2/6-31G ^{cc}	-272.863 88	-272.865 61	1.09

^a In au. ^b In kcal/mol. ^c Single point energies on RHF/3-21G optimized geometries.

and bond-breaking bond lengths in this species of 1.78 Å support that this structure corresponds to a 1,4-diyli-like species. We have used these two structures to approximate possible 1,4-diradical transition structures. In the Dupuis et al. study, this species has a C(1)–C(6) bond length of 1.641 Å,²⁸ intermediate between the UHF and the MP2 predictions.

Finally, in order to compare all three alternative pathways, the allyl radical was optimized and subjected to vibrational analysis at the UMP2/6-31G* level. This structure was used as a model for the alternative transition structure resembling two allyl radicals. The optimized structures for *C_i* symmetric 1,5-hexadiene (RHF/6-31G*), two *C_{2h}* symmetric transition structures for the concerted process (RHF/6-31G* and CASSCF/3-21G), two biradical-like structures for cyclohexane-1,4-diyli (UHF/6-31G* and MP2/6-31G*), and the allyl radical (UMP2/6-31G*) are illustrated in Figure 2.

The classic experiments by Doering and Roth on the Cope rearrangement of 3,4-dimethyl-1,5-hexadiene established that methyl groups prefer the equatorial positions in the transition state.^{1b} Further experimental work revealed that the equatorial position is preferred over the axial position by 1.5 kcal/mol in the Cope rearrangement of 3-methyl-1,5-hexadiene, and that this rearrangement occurs with an activation energy 1.3 kcal/mol lower than for the parent system, 1,5-hexadiene.^{1bj}

The theoretical treatment of the methyl-substituted Cope rearrangement involved optimizations of the reactant, product, and aromatic transition state structures for the interconversion of 3-methyl-1,5-hexadiene and *trans*-1,5-heptadiene at the RHF/6-31G* level (Figure 3). A frequency calculation was carried out at the same level on each of these stationary points.

The methyl substituent does not strongly influence the geometric or energetic features of the transition state. For example, methyl substitution at C(3) slightly lengthens both the forming and breaking bond lengths by 0.02 Å and reduces the CCC angle at C(3) from 106° to 102° in the transition state. Table II gives calculated energy differences for these two competing transition state structures with the methyl group either axial or equatorial at the RHF and MP2 levels. At the RHF/6-31G* level, the ΔE^\ddagger for the Cope rearrangement of this system is 1.5 kcal/mol lower than that for the rearrangement of 1,5-hexadiene, and the reaction is predicted to be exothermic by 3.6 kcal/mol. This computed methyl substituent effect on ΔE^\ddagger agrees well with experiment, which found this difference in activation energies to be 1.3 kcal/mol.^{1bj}

Figure 4 provides structural information for the competing axial and equatorial methyl transition structures. The view on the left shows the distance between the C(1) axial hydrogen and the C(3) axial substituent. The innermost hydrogen on the axial methyl group is significantly closer to the C(1) axial hydrogen than is the C(3) hydrogen when the methyl group is equatorial (2.243 Å vs 2.539 Å). The C(1)–C(2)–C(3) bond angle opens to accommodate this increased diaxial interaction. The lower left-hand structure shows that the methyl group arranges itself in a staggered conformation relative to C(2)–C(3) and breaking C(3)–C(4) bonds. It appears that if the innermost hydrogen were to move closer into alignment with the breaking CC bond, the diaxial interaction could be further minimized. The preference for the staggered conformation seems to override this possibility.

Theoretical Isotope Effects. The calculated kinetic and equilibrium isotope effects for the parent Cope rearrangement were computed using scaled force constants, as described in the Background. The isotope effects for the concerted aromatic

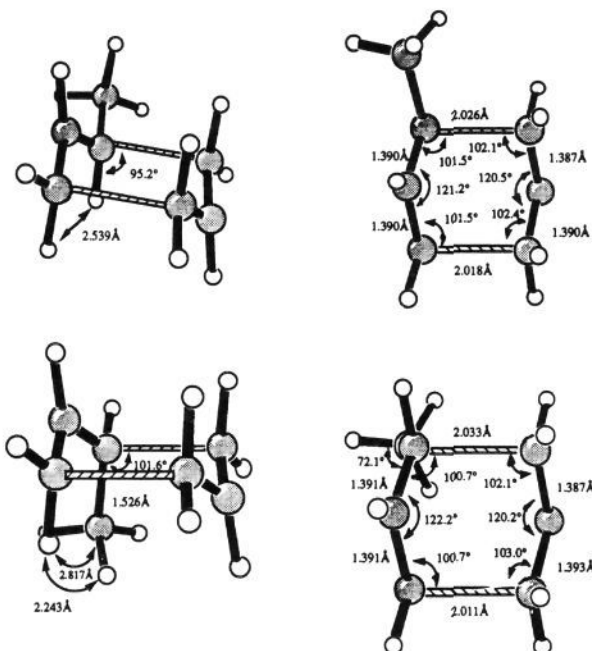


Figure 4. Two views of the transition structures for the Cope rearrangement of 3-methyl-1,5-hexadiene with methyl in the equatorial (top) and axial (bottom) positions optimized at the RHF/3-21G level.

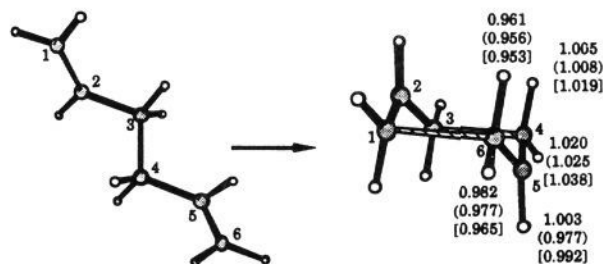


Figure 5. Kinetic isotope effects calculated for the concerted aromatic Cope rearrangement at the RHF/6-31G*, RHF/3-21G, and [CASSCF/3-21G] levels at 248 °C.

pathway were calculated at the RHF/3-21G, RHF/6-31G*, and CASSCF/3-21G levels, while those for the alternative diyl and bis-allyl pathways were calculated at the UHF/6-31G*, MP2/6-31G*, and UMP2/6-31G* levels of theory, respectively. The 1,5-hexadiene structure was vibrationally analyzed at the RHF/3-21G and RHF/6-31G* levels.

The theoretical secondary kinetic isotope effects for the concerted reaction which would result from the reaction of each possible monodeuterio-1,5-hexadiene are illustrated in Figure 5. The predictions are rather insensitive to variation in basis set, as seen by comparing RHF/3-21G values to RHF/6-31G* values. The variation due to different computational methodology is somewhat more pronounced and more systematic, with the CASSCF/3-21G values consistently 0.014–0.023 more positive than the corresponding RHF/3-21G values. As expected, the isotope effects for hydrogens at C(1) or C(6) are inverse (<1), because conversion of an sp² to an sp³ center occurs during the reaction. The effects at C(3) and C(4) are normal (>1), and those at C(2) and C(5) are quite small (≈1%).

The calculation of the isotope effect at C(3) and C(4) in 1,5-hexadiene is somewhat complex. The two methylene hydrogens attached to either of these centers in the conformationally unconstrained molecule are enantiotopic. However, when considering only the *C_i* symmetric conformation of this structure they become diastereotopic, and different force constants obtain. In the chair-like transition structure, these two hydrogens each adopt either an axial or equatorial position, again being distinct. Consideration of the evolution of the two types of methylene

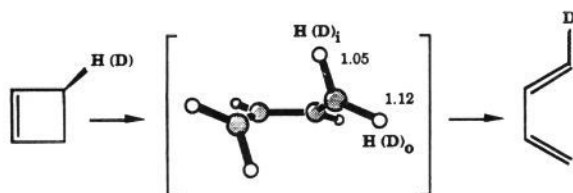


Figure 6. Theoretical kinetic isotope effects for inward and outward rotation of hydrogen in the electrocyclic ring opening of cyclobutene (ref 4b).

hydrogens into just the axial position in the chair transition state, for example, results in two distinct calculated isotope effects. However, this distinction is artificial because both of these types of hydrogens will evolve into the axial position in a conformationally mobile system. Thus, the isotope effects reported for the C(3) and C(4) positions are the geometric mean of the isotope effects for the two types of reactant sp^3 -hybridized hydrogens evolving to a single type of hydrogen in the transition state. For example, the theoretical isotope effect calculated at the RHF/6-31G* level for the conversion of the methylene hydrogen in the plane of the double bond in C_i symmetric 1,5-hexadiene to the equatorial position in the transition state is 1.024. The value for the other hydrogen participating in the same process is 1.016. The isotope effect at the equatorial position is therefore reported as $(1.024 \times 1.016)^{1/2} = 1.020$.

Note that at the bond-making centers, the isotope effect is greater for the axial hydrogen than for the equatorial hydrogen. The opposite is true for the hydrogens at the bond-breaking centers. The force constant differences between the axial and equatorial transition state C-H bonds are largely responsible, with the axial C-H bond having higher force constants. The axial C-H bond is twisted 37° out of the plane of the three-carbon moiety and is in the relatively crowded axial zone. By contrast, the equatorial C-H bond is nearly in the allyl plane ($\angle HCCC = 178^\circ$) and has force constants more like those of alkenes. Thus, for bond breaking, the larger force constant change comes with the transformation of a reactant sp^3 hydrogen to the equatorial orientation in the transition state. This results in the larger kinetic isotope effect. At the bond-making centers, the larger isotope effect results from the change of an sp^2 hydrogen to an axial hydrogen.

Baldwin and co-workers have observed a similar effect when they calculated and measured the kinetic isotope effects for the cyclobutene electrocyclic ring opening.^{4b} Figure 6 shows the calculated secondary deuterium isotope effects with no tunneling correction for hydrogen rotating inward or outward. The outer hydrogen is almost in the plane of the C(1) hydrogen, is more sp^2 -like, and has a lower bending force constant than the inner hydrogen. Accordingly, a larger kinetic isotope effect is observed experimentally and calculated theoretically for outward rotation.

Two 1,4-diyl-like "transition state" models were used for calculation of isotope effects for this mechanistic pathway. One structure is a true biradical structure, determined by UHF methodology, and the other biradicaloid type structure was located at the MP2/6-31G* level. Both are actually local energy minima, but are considered as reasonable models for a biradical-like transition state, whether or not it leads to a true biradical minimum on the potential surface. The only difference between the procedures used to calculate kinetic and equilibrium isotope effects is the multiplication of the ratio of reduced isotopic partition functions by the ratio of imaginary frequencies in the deuterated and undeuterated species (eq 3). This ratio is very close to unity and, consequently, has a minimal effect on the resulting isotope effect. For instance, in RHF/6-31G* calculations, this ratio is 1.002 for dideterio substitution at the forming and breaking bond centers. This tendency was also recently noted by Truhlar and co-workers.²⁰ As noted earlier, Dupuis, Murray, and Davidson found a pathway involving a diyl intermediate, but on the free

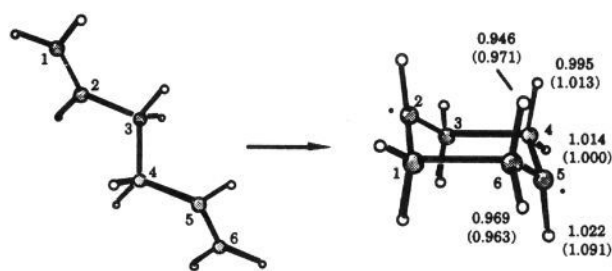


Figure 7. Theoretical secondary equilibrium isotope effects for the rearrangement of 1,5-hexadiene proceeding through a diyl-like species determined at the MP2/6-31G* and (UHF/6-31G*) levels at 248 °C.

energy surface, this is a transition state, not an intermediate.²⁸ The equilibrium isotope effects between C_i symmetric 1,5-hexadiene and the two optimized biradicaloid structures are illustrated in Figure 7.

The conversion of 1,5-hexadiene to cyclohexane-1,4-diyl involves mainly bond-forming processes between C(1) and C(6), although there is some lengthening of the C(3)-C(4) bond. Therefore, regardless of which diyl structure is chosen, the magnitudes of the isotope effects predicted at C(1), 4-5% and 3%, are significantly greater than those at C(4), which are 0.1%. Note that the same pattern obtains with regard to the axial vs equatorial positions as was found for the concerted transition state model: the axial effect is larger for bond-forming and the equatorial is the stronger effect for bond-breaking processes. Both diyl structures are predicted to have a significant normal secondary isotope effect at C(5), and this corresponds to the expected decrease in out-of-plane bending vibrational frequencies as the center changes from an alkene C-H bond to a radical C-H bond.²¹ Henderson and Pryor observed such an effect in radical additions to styrene.²² This position is the only one in the diyl where the predictions by the two computational methods differ significantly: MP2/6-31G* predicts a 2% normal secondary isotope effect, while UHF/6-31G* predicts a 9% normal effect. It is notable that the MP2/6-31G* geometry, with the relatively long C(1)-C(6) and C(3)-C(4) bonds (1.78 Å), represents a midpoint between the RHF and UHF structures. The 2% normal effect also represents an intermediate point between the very slight normal isotope effect for C(2) in the concerted structure and the 9% normal UHF/6-31G* diyl value. The electronic character of the 3-carbon fragments in the MP2 species must also fall between the delocalized system of the concerted transition state and a localized secondary radical center.

While perhaps unexpectedly large, the 9% theoretical effect predicted for C(2) in the UHF/6-31G* structure is consistent with computations of equilibrium isotope effects for other radicals, carried out at the UHF/6-31G* and CASSCF/3-21G levels.²³ If this large normal effect is in error, it could be the result of anharmonicity in the potential well not accounted for adequately by the uniform scaling procedure. A recent careful examination and comparison of experimental vibrational data and theoretical vibrational frequencies for several simple radicals suggests that at least in the case of the methyl radical the out-of-plane bending frequency may be substantially underestimated at the RHF/6-31G* level.²⁵ Were this the case for the cyclohexane-1,4-diyl then the magnitude of the theoretical isotope effect at the radical center would be exaggerated. A tunneling correction, applied to the k_H/k_D ratio assuming a parabolic potential surface, did not

(21) Pacansky, J.; Miller, M. D.; Koch, H. *J. Am. Chem. Soc.* **1991**, *113*, 317-43.

(22) Henderson, R. W.; Pryor, W. A. *Int. J. Chem. Kinet.* **1972**, *4*, 325-330.

(23) CASSCF/3-21G, 4 electron and 4 orbital active space calculations on ethyl radical and 2-hexene-1,6-diyl also predict relatively large deuterium secondary kinetic isotope effects for the transformation of a vinylic C-H to a primary radical.

(24) (a) Humski, K.; Malojčić, R.; Borčić, S.; Sunko, D. *J. Am. Chem. Soc.* **1970**, *92*, 6534-38. (b) Humski, K.; Strelkov, T.; Borčić, S.; Sunko, D. *E. J. Chem. Soc. D* **1969**, 693-94.

(25) Pacansky, J.; Koch, W.; Miller, M. D. *J. Am. Chem. Soc.* **1991**, *113*, 317-328.

(20) Lu, D.-H.; Maurice, D.; Truhlar, D. *J. Am. Chem. Soc.* **1990**, *112*, 6206-14.

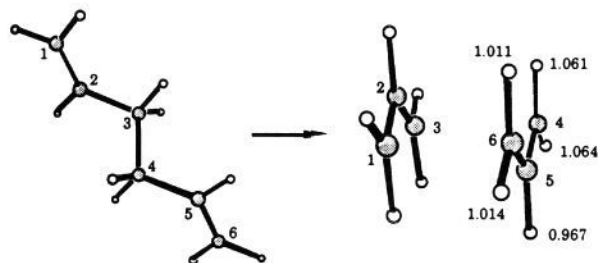


Figure 8. Theoretical secondary kinetic isotope effects for the rearrangement of 1,5-hexadiene proceeding through two allyl radical fragments at 248 °C. The allyl radical was optimized at the UMP2/6-31G* level.

Table III. Calculated and Experimental Bond-Breaking Equilibrium Isotope Effects (EIE) for the Cope Rearrangement of 3,3,4,4-Tetradeuterio-1,5-hexadiene

T(°C)	expt	RHF/3-21G	RHF/6-31G*	MP2/6-31G*
150	1.27 ^a	1.37	1.34	1.36
200	1.24 ^a	1.28	1.26	1.27
218	1.21 ± 0.03 ^b	1.26	1.24	1.25

^a Taken from ref 24. ^b Taken from ref 5a.

significantly change the value (<0.2%).²⁶

Isotope effects for the hypothetical cleavage-recombination pathway via two allyl radicals are illustrated in Figure 8. Note that the isotope effects at both the bond-breaking and subsequent bond-forming positions are normal. This is due to the fact that the out-of-plane bending force constants at the termini of the allyl radical are smaller than those at either the sp²- or sp³-hybridized centers. Both monodeuterio kinetic isotope effects at the bond-breaking center are large (6%), while those at the other terminus are only 1% at this relatively high temperature.

Comparison with Experiment. Table III lists the calculated and experimental equilibrium isotope effects for bond breaking in the Cope rearrangement at three different temperatures. The rearrangement is degenerate, so the equilibrium isotope effects for bond formation are simply the inverse of the bond-breaking effects. The experimental results reported in ref 24 do not include error limits. However, the 6-31G* result is within the error limits given in ref 5a.

Gajewski has measured the kinetic isotope effects for the Cope rearrangement of 1-methyl- and 3-methyl-1,5-hexadiene.⁵ The results are shown in Table IV along with the theoretical kinetic isotope effects calculated for the concerted Cope rearrangement of the parent and methyl-substituted 1,5-hexadienes. The isotope effects per hydrogen are shown in brackets.

At the RHF/6-31G* level, the theoretical bond-making and bond-breaking kinetic isotope effects for 4,4-dideuterio-3-methyl-1,5-hexadiene are 0.95 and 1.03. The per hydrogen values are 0.97 and 1.02, respectively. These results are in exact agreement with the corresponding experimental values (entries 2 and 6 of Table IV). In nearly all cases the calculated kinetic isotope effects are within the experimental error range, with only entry 5 out of line. Indeed, the authors had noted in the paper that this result was probably in error.^{5a} Also note that the per hydrogen isotope effect for this entry differs significantly from the other bond-breaking measurements.

A summary of the theoretical and experimental kinetic isotope effects is provided in Figure 9. Note that while the values for the concerted mechanism are within the experimental error, the kinetic isotope effects for either 1,4-diyl transition state model fall outside of this range, and the values indicate somewhat more bond making and less bond breaking than the experimental values support. The computed result for bond making in the allyl radical pathway is inverse relative to that of experiment and is indicative of much more bond breaking than found in the values measured experimentally.

Table IV. Experimental and Theoretical Kinetic Isotope Effects for the Cope Rearrangement at 248 °C. The Theoretical Results are Given for the Concerted Aromatic Mechanism at the RHF/6-31G* and (RHF/3-21G) Levels

Reactant	3-methyl-1,5-hexadiene		
	Experimental ^a	RHF/6-31G* (RHF/3-21G)	1,5-hexadiene RHF/6-31G* (RHF/3-21G)
(1)	0.89 ± 0.018	0.90 (0.87)	0.89 (0.87)
(2)	[0.97] ^b	[0.97]	[0.97]
(3)	0.95 ± 0.019	0.95 (0.94)	0.94 (0.93)
(4)	[0.97]	[0.97]	[0.97]
(5)	0.96 ± 0.003	0.95 (0.94)	0.94 (0.93)
(6)	[0.98]	[0.97]	[0.97]
(7)	1.07 ± 0.025	1.05 (1.07)	1.05 (1.07)
(8)	[1.02]	[1.01]	[1.01]
(9)	1.09 ± 0.027	1.03 (1.03)	1.03 (1.03)
(10)	[1.04]	[1.02]	[1.02]
(11)	1.03 ± 0.019	1.03 (1.04)	1.03 (1.03)
(12)	[1.02]	[1.02]	[1.02]

^a Gajewski notes that errors in the rate constants for the rearrangement of 1-methyl-1,5-hexadiene, entries 3, 4, and 5, are probably larger than that indicated by the error margins reported above.^{5a} ^b The isotope effects per hydrogen are shown in brackets for comparison. For the theoretical results, this value refers to the RHF/6-31G* calculation.

Table V. Calculated (AM1) and Experimental Kinetic Isotope Effects for Bond Breaking (BB) and Bond Making (BM) in the Cope Rearrangement of 3,3,4,4-Tetradeuterio-1,5-hexadiene and 1,1,6,6-Tetradeuterio-1,5-hexadiene, Respectively

	T(°C)	KIE (BM)	KIE (BB)
AM1 ^a			
biradicaloid	250	0.88	1.00
aromatic	250	0.88	1.03
expt ^b	248	0.89 ± 0.02	1.07 ± 0.03

^a Taken from ref 3d. ^b For the Cope rearrangement of 3-methyl-1,5-hexadiene, taken from ref 5a.

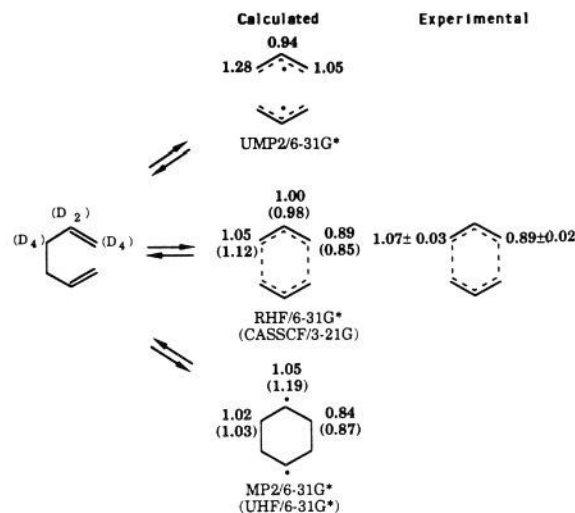


Figure 9. Experimental and calculated kinetic isotope effects for three alternative pathways for 1,1,6,6-tetradeuterio-1,5-hexadiene (bond making), 3,3,4,4-tetradeuterio-1,5-hexadiene (bond breaking), and 2,5-dideuterio-1,5-hexadiene at 248 °C. Experimental data are from entries 1 and 4 in Table IV.

Dewar and co-workers have calculated the kinetic isotope effects for the Cope rearrangement of [1,1,6,6- and [3,3,4,4-²H]-1,5-hexadiene using semiempirical calculations at the AM1 level.^{3c-e} Two chair-like transition states were located, a biradicaloid and

(26) Bell, R. P. *The Proton in Chemistry*; 2nd ed.; Chapman and Hall: New York, 1973, Vol. 19, 275-277.

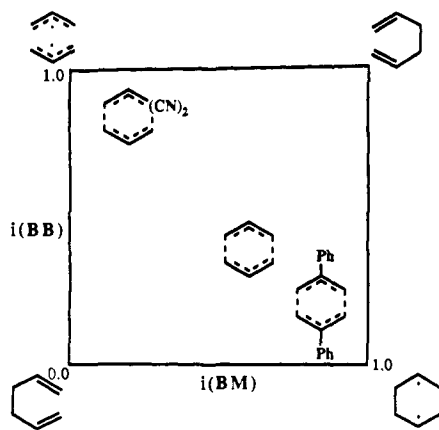


Figure 10. A qualitative More O'Ferrall-Jencks diagram for the transition states of three Cope rearrangements.^{5a}

an aromatic transition state. The calculated isotope effects at the bond-forming and bond-breaking positions are given in Table V. As can be seen, neither set of isotope effects for bond breaking falls within the experimental range of error, in spite of being cited as in good agreement with experiment. The results of the AM1 calculations on both the concerted and biradicaloid pathways indicate significantly less bond breaking than revealed by experiment.

The Classification of Transition State Structure through More O'Ferrall-Jencks Diagrams. One goal of this work is to contribute to the development of a quantitative relationship between kinetic isotope effects and some measure of bonding and geometric changes occurring at the reacting center. Gajewski⁵ and co-workers have used More O'Ferrall-Jencks²⁷ (MOJ) diagrams to correlate graphically the experimentally determined secondary deuterium isotope effects with the relative extent of bonding changes at the reacting centers in the transition states of [3,3]-sigmatropic rearrangements.

A number of important assumptions have been made to proceed with developing these diagrams for this particular reaction. (1) Equilibrium isotope effects, for the individual bond-making or bond-breaking processes, are assumed to be the maximum possible isotope effect. The value of the isotope effect for isotopic substitution at a particular position is assumed to correspond to complete progress along the reaction pathway. It follows that a kinetic isotope effect for the actual process will be some fraction of the equilibrium isotope effect and is in some way proportional to the degree of change at the substituted center. (2) The isotope effect is assumed to be related directly to the change in σ bond order in proceeding from the ground state to the transition state. Therefore, the relationship between the kinetic and equilibrium isotope effects can be used to assess the degree of σ bond change in the transition state. As a point of departure, Gajewski has proposed a linear free energy relationship. The index of bond making $i(\text{BM})$ and bond breaking $i(\text{BB})$ is defined as the logarithm of the kinetic isotope effect divided by the logarithm of the equilibrium isotope effect.^{5f}

$$i(\text{BM}) = \frac{\ln(\text{KIE})_{\text{BM}}}{\ln(\text{EIE})_{\text{BM}}} \quad i(\text{BB}) = \frac{\ln(\text{KIE})_{\text{BB}}}{\ln(\text{EIE})_{\text{BB}}}$$

The kinetic isotope effect is derived from experiment, and the equilibrium isotope effect is derived from fractionation factors.

A typical More O'Ferrall-Jencks diagram, derived from Gajewski's experimental work, is illustrated in Figure 10. It provides a graphic comparison of the transition states for the Cope rearrangements of the parent compound and two substituted derivatives. The reactant is in the lower left corner, the product is in the upper right, and the horizontal and vertical axes indicate the bond index for the making and breaking σ bonds, respectively.

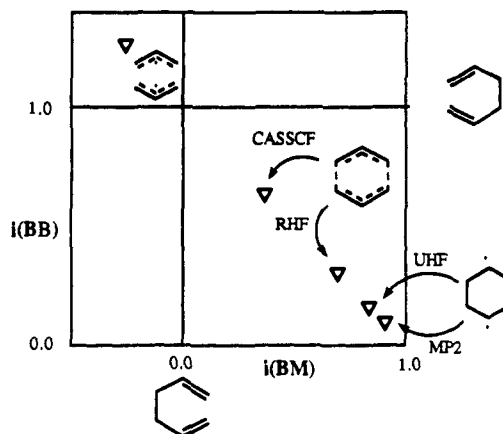


Figure 11. The MOJ diagram based on theoretical isotope effects illustrating the bond-making, bond-breaking, and concerted pathways.

The transition state sketches also mark the approximate locations of each of these on the diagram.

The parent system is near the center of the diagram. Diphenyl substitution at C(2) and C(5) shifts the transition state toward the 1,4-diyl species in the lower right corner, while 3,3-dicyano substitution yields a transition state resembling more closely two allyl radicals in the upper left corner.

Use of this model to illustrate the results reported here for the possible alternative transition structures for the parent Cope reaction reveals a complication. The diagram in Figure 11 shows the locations of the theoretical concerted (RHF/6-31G* and CASSCF), 1,4-diyl (UHF/6-31G* and MP2/6-31G*), and allyl radical (UMP2/6-31G*) transition structures on a MOJ diagram. The indices, $i(\text{BM})$ and $i(\text{BB})$, are calculated using theoretical values for the KIE, and the EIE is derived from fractionation factors. The concerted transition state structure falls near the center of the diagram, displaced somewhat to the lower right corner. Both 1,4-diyl transition structures are located close to the lower right-hand corner of the diagram, as expected. The theoretical transition state resembling two separate allyl radicals should be located in the upper left corner of the diagram. However, to include this transition state the usual MOJ diagram bond-breaking and bond-forming axes must be extended beyond the normal 0–1.0 range.

The problem with incorporating the results for a bis-allyl radical transition state is 2-fold. The UMP2/6-31G* calculations indicate that a transition state with such a large degree of bond-breaking character would yield very strong normal kinetic isotope effects at the bond-breaking centers. It is, in fact, larger than the corresponding equilibrium isotope effect. When Gajewski's equation is used, this situation yields a bond-breaking index greater than unity. The same calculations predict a smaller, but still normal, kinetic isotope effect at what will ultimately be the bond-making centers, C(1) and C(6). The bond-making equilibrium isotope effect at this position is inverse. The resulting Gajewski bond index is therefore negative ($i = -0.26$). This illustrates a general problem in the assumption that a fractionation factor, or equilibrium isotope effect, can be used as the upper limit for the corresponding kinetic isotope effect for a given process.

There are a variety of ways in which this problem can be handled. By the use of more complicated functions, the upper left corner of a square diagram could represent two allyl radicals (both bond indices = 0), but each axis would then represent a reaction coordinate which is a function of both bond making and bond breaking.²⁸

Relationship of the Bond Index, i , to Bond Order. For the MOJ diagrams to carry information about structure as related to isotope effect, the bond index parameter should be replaced with a measure of the geometry of the transition structure. The bond

(27) (a) More O'Ferrall, R. A. *J. Chem. Soc. B* 1970, 274–77. (b) Jencks, W. P. *Chem. Rev.* 1972, 72, 705–18.

(28) See, for example: Gajewski, J. J.; Olson, L. P.; Tupper, K. J., submitted for publication.

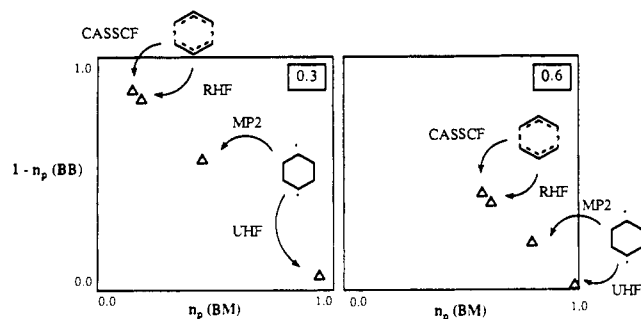


Figure 12. More O'Ferrall-Jencks diagrams of the concerted and 1,4-diyl pathways for the Cope rearrangement of 1,5-hexadiene, with coordinates defined using modified Pauling bond orders and constants of 0.3 or 0.6.

order is usually defined as a function of bond length.²⁹ The commonly used Pauling bond order, n_p , is defined in eq 4, where n_0 is the bond order of the fully formed bond of length R_0 , and R is the length of a bond with bond order n_p .

$$n_p = n_0 \exp \left[\frac{(R_0 - R)}{0.3} \right] \quad (4)$$

More recently, the Indiana group has found that a proportionality constant of 0.6 (rather than 0.3) is more appropriate for cases where the bond in question is of bond order less than 1 (eq 5).³⁰

$$n_p = n_0 \exp \left[\frac{(R_0 - R)}{0.6} \right] \quad (5)$$

For the regions of bond order between 1 and 3, commonly discussed by Pauling, n_p is not altered significantly by this change of constant.^{29c} The value of $n = 0.3$ is normally maintained for

(29) (a) Pauling, L. *J. Am. Chem. Soc.* **1947**, *69*, 542-53. (b) Gordy, W. *J. J. Chem. Phys.* **1947**, *15*, 305. (c) Paolini, J. P. *J. Comput. Chem.* **1990**, *11*(10), 1160-63.

(30) Personal communication with J. J. Gajewski, based upon work with E. R. Davidson and V. J. Shiner.

$n_p > 1$. The Pauling bond order using 0.3, as well as other bond orders, such as those proposed by Gordy and Paolini, do not give reasonable values of bond orders for very long bonds.

A bond order MOJ diagram can be defined with the bond-making axis equal to $n_p(\text{BM})$ and the bond-breaking axis equal to $[1 - n_p(\text{BB})]$. The partial bond order indices are calculated using eqs 4 or 5 from the bond lengths of the transition state structures generated in this study. The bond length R_0 (which corresponds to zero bond breaking and complete bond making) is the C(3)-C(4) bond length in 1,5-hexadiene, 1.539 Å. The concerted transition state and two 1,4-diyl transition structures are presented in this manner in Figure 12. Bond orders derived from the original Pauling equation, eq 4, indicate a great deal more bond breaking than bond making in the concerted Cope transition state, while the 1,4-diyl lies near the middle of the diagram. When eq 5 is used, the locations of both structures are considerably closer to that predicted by the Gajewski-type MOJ diagram. However, there is still relatively more bond breaking indicated for both the concerted and 1,4-diyl transition state than indicated from the isotope effect derived bond indices. Qualitatively, both types of diagrams give similar information about the shift in the nature of the transition states as a function of calculation type, or as proposed by Gajewski as a function of substituents.

Conclusion

Theoretical secondary kinetic isotope effects derived from ab initio frequency calculations have been correlated with experimental results to differentiate between competing mechanistic pathways for the Cope reaction. These results support a mechanism involving concerted bond reorganization in the transition state.

Acknowledgment. We are grateful to the National Science Foundation for financial support of this research and to Professors Martin Saunders, Joseph J. Gajewski, V. J. Shiner, Jr., and Weston T. Borden for helpful discussions. We also would like to thank the UCLA Office of Academic Computing for their generous allocation of IBM 3090 computing resources.

Registry No. $\text{H}_2\text{C}=\text{CH}(\text{CH}_2)_2\text{CH}=\text{CH}_2$, 592-42-7; $\text{H}_2\text{C}=\text{CH}(\text{C}-\text{H}_2)_3\text{CH}=\text{CH}_2$, 1541-23-7; $\text{H}_2\text{C}=\text{CHCH}(\text{CH}_3)\text{CH}_2\text{CH}=\text{CH}_2$, 1541-33-9; D_2 , 7782-39-0.